

# Linköping University Post Print

## **Radio-frequency lesioning in brain tissue with coagulation-dependent thermal conductivity: modelling, simulation and analysis of parameter influence and interaction**

Johannes D Johansson, Ola Eriksson, Joakim Wren, Dan Loyd and Karin Wårdell

N.B.: When citing this work, cite the original article.

The original publication is available at [www.springerlink.com](http://www.springerlink.com):

Johannes D Johansson, Ola Eriksson, Joakim Wren, Dan Loyd and Karin Wårdell, Radio-frequency lesioning in brain tissue with coagulation-dependent thermal conductivity: modelling, simulation and analysis of parameter influence and interaction, 2006, Medical and Biological Engineering and Computing, (44), 9, 757-766.

<http://dx.doi.org/10.1007/s11517-006-0098-1>

Copyright: Springer Science Business Media

<http://www.springerlink.com/>

Postprint available at: Linköping University Electronic Press

<http://urn.kb.se/resolve?urn=urn:nbn:se:liu:diva-15926>

## **Radio-Frequency Lesioning in Brain Tissue with Coagulation-Dependent Thermal Conductivity – Modelling, simulation and analysis of parameter influence and interaction**

Johannes D. Johansson<sup>1</sup>, Ola Eriksson<sup>1,2</sup>, Joakim Wren<sup>3</sup>, Dan Loyd<sup>3</sup> and Karin Wårdell<sup>1</sup>

<sup>1</sup>Department of Biomedical Engineering, Linköping University, Linköping, Sweden

<sup>2</sup>Elekta Instrument AB, Sweden

<sup>3</sup>Department of Mechanical Engineering, Linköping University, Linköping, Sweden

Corresponding author: J. Johansson, Department of Biomedical Engineering, Linköping University, SE-581 85 Linköping, Sweden (e-mail: johjo@imt.liu.se; phone: +46 13-222464; fax: +46 13-101902;).

This work was supported by The Swedish Research Council (Vetenskapsrådet, No. 621-2002-5772) and NIMED (Competence Center Noninvasive Medical Measurements).

### **Abstract**

Radio-frequency brain lesioning is a method for reducing e.g. symptoms of movement disorders. A small electrode is used to thermally coagulate malfunctioning tissue. Influence on lesion size from thermal and electric conductivity of the tissue, microvascular perfusion and preset electrode temperature was investigated using a finite element model. Perfusion was modelled as an increased thermal conductivity in non-coagulated tissue. The parameters were analysed using a 2<sup>4</sup>-factorial design (n=16) and quadratic regression analysis (n=47). Increased thermal conductivity of the tissue increased lesion volume, while increased perfusion decreased it since coagulation creates a thermally insulating layer due to the cessation of blood perfusion. These effects were strengthened with increased preset temperature. The electric conductivity had negligible effect. Simulations were found realistic compared to in vivo experimental lesions.

## **Keywords**

Electrosurgery, RF-ablation, Brain, Blood perfusion, Finite Element Method,

## **Introduction**

Thermocoagulation using a radio-frequency (RF) current, i.e. RF-lesioning or RF-ablation, is a widely used therapy for e.g. cardiac arrhythmias (Tungjitkusolmun et al. 2000), liver tumours (Goldberg 2001), severe chronic pain and brain disorders such as Parkinson's disease (Cosman 1996). For these surgical procedures, the final lesion size depends on several parameters such as electrode design, RF-generator settings and the characteristics of the tissue in the target area. During lesioning in the brain, a relatively small electrode is stereotactically guided into the central part of the brain, and a lesion is created by the temperature increase in the tissue surrounding the electrode tip caused by the RF-current. For an optimal outcome of such an intervention, the pre-planning procedure, the target definition and the size and shape of the lesion are of importance. The knowledge about the lesion development and its final size and shape is today limited during surgery, although the size can be roughly estimated post-operatively by magnetic resonance imaging (MRI) or computed tomography (CT) (De Salles et al. 1995), (Hariz and Hirabayashi 1997).

A possible step in the improvement of predictability and control during the RF-lesioning process is computer simulation, preferable on an individual patient basis. In previous studies we have modelled a brain electrode, using the finite element method (FEM), where the output power from the RF-generator was modelled as various spatially piecewise constant heat sources in the tissue around the electrode tip. This model was compared to in-vitro lesions generated in a protein solution (Eriksson et al. 1999). Furthermore, we investigated the temperature variations around the electrode tip during lesioning using this model (Wren et al. 2001a). In the current investigation we use a refined simulation of the spatial power distribution around the electrode tip and have also taken coagulation of the tissue and resulting cessation of blood perfusion into account. A central issue in the modelling of thermocoagulation, as well as all other thermal treatments, is to account for the thermal effect of blood flow perfusion. The perfusion

both drains heat from, and disperses heat within, the target area. This affects the temperature level and distribution and thus ultimately the result of the thermal treatment. The thermocoagulation simulated in this paper is carried out in the central grey of the brain, e.g. the thalamus or globus pallidus, where microcirculation is predominant. For such perfusion, the blood is very close to thermal equilibrium with the surrounding tissue (Chato 1980) and it has been found that the thermal effects of blood perfusion under this condition can be modelled accurately by the effective conductivity model (Wren 2002), (Weinbaum and Jiji 1989).

The aim of this study was to investigate the influence on the lesion size from the thermal and electrical conductivity of the tissue, the microvascular blood perfusion and the preset electrode temperature and their interactions. Perfusion was modelled as an increased thermal conductivity. In this study a coagulation dependency of this parameter was introduced, since the perfusion ceases in coagulated tissue. The influence and interaction between all these parameters were investigated using factorial design and regression analysis.

## **Material and Methods**

The temperature distribution and the lesion size have been simulated using the finite element method. A statistical design of the simulations has been used to investigate the effect of blood perfusion, electric and thermal conductivities, target temperature and their interactions on lesion volume.

### ***The RF-system***

In this study a model of a monopolar brain electrode (Elekta Instrument AB, Sweden) was set-up in order to investigate the thermal interaction with the surrounding tissue. The electrode, made of stainless steel, has a diameter of 1 mm and an active tip length of 4 mm separated from the upper electrode body by an electrically insulating layer of 2 mm (Fig. 1a). During RF-lesioning, the electrode is connected to a current generator (Leksell<sup>®</sup> Neuro Generator (LNG), Elekta Instrument AB, Sweden), which supplies and controls the RF-current (512 kHz). The temperature is continuously recorded by a thermocouple

positioned inside the electrode tip ( $T_{tip}$ ), in order to perform lesions using a preset temperature and to avoid boiling of the tissue. The LNG also limits the rate of heating to a maximum of 6 °C/s. Common preset temperatures ( $T_{set}$ ) on the LNG used for lesioning in brain tissue are 70, 80 and 90 °C.

### ***Governing Equations***

Equations for steady current and time-dependent conductive heat transfer were used, together with appropriate boundary conditions, in order to simulate the lesioning. In this case the equations are dependent on each other and should be solved together. The resistive heating with coagulation-dependent effective thermal conductivity is presented below.

#### *Steady Current*

In RF-surgery the frequency is low enough for quasi-stationarity since the electric wavelength is much larger than the geometrical dimensions of interest (Labonté 1992) and further the impedance of the tissue can be assumed to be purely resistive during heating (van den Berg and van Manen 1962). Therefore the frequency is only considered to affect the electric conductivity of the tissue and the electric field around the electrode can thus be calculated using the relation for steady current (Cheng 1989):

$$\nabla \cdot \mathbf{J} = -\nabla \cdot (\sigma(T) \nabla V) = 0 \quad (\text{A/m}^3) \quad (1)$$

In Eq. (1),  $\mathbf{J}$  denotes the electric current density ( $\text{A/m}^2$ ),  $\sigma(T)$  the electric conductivity ( $\text{S/m}$ ) at tissue temperature  $T$  ( $^{\circ}\text{C}$ ) and  $V$  corresponds to the electric potential ( $\text{V}$ ). The electric conductivity of the tissue is assumed to depend on the temperature of the tissue by an increase of 1.75 % per  $^{\circ}\text{C}$  above 20  $^{\circ}\text{C}$ . This assumption is known to be valid for temperatures between 20 and 40  $^{\circ}\text{C}$  at frequencies below 50 MHz (Duck 1990).

#### *Heat Conduction*

Unsteady conductive heat transfer can be described by the heat conduction equation (Carslaw and Jaeger 1959):

$$\rho c \frac{\partial T}{\partial t} = \nabla \cdot (k \nabla T) + \dot{Q} \quad (\text{W/m}^3) \quad (2)$$

In (2), the mass density is denoted by  $\rho$  (kg/m<sup>3</sup>), the specific heat capacity by  $c$  (J/(kg·K)), the time by  $t$  (s), the thermal conductivity by  $k$  (W/(m·K)) and the power density by  $\dot{Q}$  (W/m<sup>3</sup>).

#### *Resistive Heating with Coagulation-Dependent Effective Thermal Conductivity*

The temperature distribution around the electrode is calculated using the heat conduction equation with resistive heating as the power source according to:

$$\dot{Q} = \sigma(T) (\nabla V)^2 \quad (3)$$

In order to mimic the power control of the LNG the power source must be turned off when  $T_{tip}$  exceeded  $T_{set}$ . Combining Eq. (2) and (3) and regulation of the power gives the following relation for the brain tissue:

$$\rho c \frac{\partial T}{\partial t} = \begin{cases} \nabla \cdot (k_{tiss} \nabla T) + \sigma(T) (\nabla V)^2 & (T_{tip} \leq T_{set}) \\ \nabla \cdot (k_{tiss} \nabla T) & (T_{tip} > T_{set}) \end{cases} \quad (\text{W/m}^3) \quad (4)$$

In Eq. (4),  $k_{tiss}$  denotes the thermal conductivity (W/(m·K)) of the brain tissue.

In this study we are interested in simulating the influence on lesion size from several parameters of which one is microvascular perfusion. Equation (4), however, does not take blood perfusion into account. The blood perfusion for a general tissue with varying vessel sizes can be described by the hybrid bio-heat equation (Wren et al. 2001b). With the assumption of only microcirculation (vessel diameter less than approximately 200  $\mu\text{m}$ ) which should be appropriate in the central part of the brain, the hybrid bio-heat equation is reduced to the effective conductivity equation (Wren et al. 2001a). Perfusion is then modelled by increasing  $k_{tiss}$  by a term roughly proportional to the blood perfusion ( $k_{perf}$ ) (Raaymakers et al. 2000). The sum of  $k_{tiss}$  and  $k_{perf}$  is denoted the effective thermal conductivity ( $k_{eff}$ ). Furthermore, the microvessels are considered to be in thermal

equilibrium with the surrounding tissue (Chato 1980) and should coagulate when the temperature of the tissue reaches approximately 60 °C ( $T_{coag}$ ), thus ceasing the blood flow. In order to introduce a coagulation-dependent term,  $k_{eff}$  must also include a temperature-dependent  $k_{perf}$ -term. Combining the above assumptions results in the governing equations for resistive heating with coagulation-dependent effective thermal conductivity:

$$\rho c \frac{\partial T}{\partial t} = \begin{cases} \nabla \cdot (k_{eff} \nabla T) + \sigma(T)(\nabla V)^2 & (T_{tip} \leq T_{set}) \\ \nabla \cdot (k_{eff} \nabla T) & (T_{tip} > T_{set}) \end{cases} \quad (\text{W/m}^3) \quad (5)$$

where

$$k_{eff} = \begin{cases} k_{tiss} + k_{perf} & (T \leq T_{coag}) \\ k_{tiss} & (T > T_{coag}) \end{cases} \quad (\text{W/(m}\cdot\text{K)}) \quad (6)$$

### ***Finite Element Model***

An axi-symmetrical model of a temperature-controlled stainless steel electrode with a diameter of 1 mm and an active tip length of 4 mm was implemented together with Equations (1), (5) and (6) in a finite element program (FEMLAB 2.3, Comsol AB, Sweden) using a PC (1700 MHz, 1024 MB). The tip was separated from the rest of the electrode by an electrically insulating plastic layer. A sphere of homogeneous grey matter with a radius of 30 mm surrounded the electrode. A voltage of 25 V was assigned to the electrode tip and the surface of the sphere was assigned as ground. The sphere was made large compared to the electrode tip in order to have ground sufficiently far away so its exact location and size does not seriously affect the electric field around the tip. The surface was also assumed to hold a constant temperature of 37 °C. It was assumed that the current from the tip was confined to the tissue and that no current flowed back through the electrode. For each time-step the software determines whether the tip temperature  $T_{tip}$  has reached the preset temperature  $T_{set}$  or not, delivering power only in steps where  $T_{set} \geq T_{tip}$ . The power control was implemented in Eq. (5) instead of controlling the voltage of the electrode tip since the time stepping algorithms of the

software considers time varying subdomain settings but ignores time varying boundary conditions. This would give very poor simulation results if the latter were used. Equations (5) and (6) were implemented using a differentiable version of Heaviside's step function in the software. A mesh of 3 847 elements was used for the simulations. Simulations were performed for a corresponding lesioning time of 60 s. A lesion in the simulation was assumed to consist of all tissue at  $T > 60$  °C and its volume and maximum diameter were computed. The model set-up is described in Fig. 1b and the physical properties of the different material are given in Table I.

### ***Simulation Design and Statistical Analysis***

Simulations were carried out in order to investigate the influence on lesion volume and diameter from the thermal and electric conductivity of the tissue as well as the microvascular perfusion and the preset lesioning temperature. These parameters were varied using a preliminary factorial design and then a refining quadratic regression analysis (Montgomery 1996) with corresponding contrast coefficients denominated  $\mathbf{c}_\sigma$ ,  $\mathbf{c}_{\text{ktiss}}$ ,  $\mathbf{c}_{\text{kperf}}$  and  $\mathbf{c}_{\text{Tset}}$  respectively. The levels (low, semi-low, mean, semi-high, high) and corresponding values for the contrast coefficients are given in Table II. Only low (-1) and high (+1) levels were used for the factorial design.

The simulations were performed in two steps. First a  $2^4$ -factorial design (n=16, Table III) was performed and a normal probability plot was used in order to find the important effects on lesion volume. Unimportant effects will align in an approximately straight line in a normal probability plot, while important effects will deviate from the normal distribution. Effects from multiples of three or more variables are seldom significant and non-significant effects were excluded in the regression model. A centre point simulation was then carried out with all factors at the mean level and the result was compared to the regression model in order to evaluate the linearity of the model.

As the regression model based on the  $2^4$ -factorial design was found insufficient more simulations were carried out in order to obtain a quadratic regression model (total n=47). As a result of the factorial design, the electric conductivity was now omitted as an

explanatory factor and was set to 0.175 S/m (mean level) in the additional simulations. The remaining variables were varied at five different levels (Table II) according to design matrix C (Table IV).

The regression analysis was performed using MatLab 6.5 (MathWorks Inc., USA), which also calculates the double-sided confidence intervals for the regression coefficients, residual standard deviation  $s$  and proportion of variability explained by the regression model  $R^2$ . Non-significant coefficients were removed one at a time through backward elimination (Montgomery and Runger 1994), removing the coefficient with poorest significance in every iteration, until all coefficients in the regression model were significant at  $p < 0.005$ .

## Results

In order to visualize the coagulation dependent thermal conductivity, two examples of the simulated lesions with and without blood perfusion are presented in Fig. 2 together with a plot of the resulting effective thermal conductivity of the tissue.

### *2<sup>4</sup>-Factorial Design*

The resulting volumes and diameters for the 2<sup>4</sup>-factorial design are given in Table III and the important effects on the volume between temperature, thermal and electrical conductivity, and blood perfusion presented in the normal probability plot in Fig. 3. It is seen that  $T_{set}$ ,  $k_{tiss}$  and the interaction between  $T_{set}$  and  $k_{tiss}$  increased the simulated volume while  $k_{perf}$  and interaction between  $T_{set}$  and  $k_{perf}$  decreased it. The effect of the electric conductivity ( $\sigma$ ) was negligible, and was thus not included in the refined study. Using only the important effects, results in the following regression model:

$$\begin{aligned}
 Volume = & 49.3 + 28.2 \left( \frac{T_{set} - 80}{10} \right) + 8.3 \left( \frac{k_{tiss} - 0.35}{0.15} \right) - 17.9 \left( \frac{k_{perf} - 0.25}{0.25} \right) \\
 & + 5.5 \left( \frac{T_{set} - 80}{10} \right) \left( \frac{k_{tiss} - 0.35}{0.15} \right) - 10.4 \left( \frac{T_{set} - 80}{10} \right) \left( \frac{k_{perf} - 0.25}{0.25} \right) \quad (\text{mm}^3) \quad (7)
 \end{aligned}$$

with  $s = 2.0$  and  $R^2 = 98.8\%$  ( $p < 0.0001$ ). The 95 % confidence intervals for all effects and the mean value are  $\pm 1.1 \text{ mm}^3$ . The effects are visualised in Fig 4. The prediction from Eq. (7) differs from the result from the centre point simulation at mean level of all factors by about  $9 \text{ mm}^3$  (49.3 compared to  $40.2 \text{ mm}^3$ , see Table III). This is a difference of more than four times the estimated standard deviation,  $s$ , compared to the model. As can be seen in Fig. 4a, this gives a curvature that indicates that higher order terms may improve the regression model.

### ***Quadratic Regression Model***

The resulting volumes and diameters for the quadratic regression design ( $n = 47$ ) can be seen in Table IV and resulted in the following regression model for the volume:

$$\begin{aligned}
 \text{Volume} = & 42.1(\pm 1.1) + 24.9(\pm 1.5) \left( \frac{T_{set} - 80}{10} \right) + 8.2(\pm 0.7) \left( \frac{k_{tiss} - 0.35}{0.15} \right) \\
 & - 17.8(\pm 0.7) \left( \frac{k_{perf} - 0.25}{0.25} \right) + 6.6(\pm 0.9) \left( \frac{k_{perf} - 0.25}{0.25} \right)^2 + 5.7(\pm 0.9) \left( \frac{T_{set} - 80}{10} \right) \left( \frac{k_{tiss} - 0.35}{0.15} \right) \\
 & - 10.6(\pm 1.3) \left( \frac{T_{set} - 80}{10} \right) \left( \frac{k_{perf} - 0.25}{0.25} \right) + 3.6(\pm 1.7) \left( \frac{T_{set} - 80}{10} \right) \left( \frac{k_{perf} - 0.25}{0.25} \right)^2
 \end{aligned} \quad (\text{mm}^3) \quad (8)$$

with  $s = 1.9$  and  $R^2 = 99.6\%$  ( $p < 0.0001$ ). The numbers in parentheses behind the coefficients in Eq. 8 show the 95 % confidence interval. Visualisation of the interaction between preset temperature and thermal conductivity as well as between temperature and blood perfusion on the lesion volume are presented in Fig. 5a and b respectively where the increased effect with  $T_{set}$  and curvature for  $k_{perf}$  clearly can be seen.

### **Discussion**

In this study, a FEM model of RF-lesioning in brain tissue was set up using resistive heating and a heat conduction equation with coagulation-dependent effective thermal conductivity. In such an implementation, both the heat transfer equation and the equation for steady state current are solved together. Electric and thermal conductivity, target

temperature and blood perfusion were varied in order to investigate their impacts on the resulting volume and diameter of simulated RF-lesions. The effect of blood perfusion was modelled as an increase of the effective thermal conductivity in non-coagulated tissue. The electric and thermal conductivity were included as variables since tabulated values from different experimental studies can vary considerably (see Table I).

Factorial designs are very useful for finding important variables and interactions between them, while limiting the amount of data needed. They are widely used when designing experiments and should always be considered when several possible variables are present, since it is easy to miss important interactions if variables are examined one at a time (Montgomery 1996). The results can then, as in this study, be used to make more advanced designs using only the important factors. Factorial designs can also be very appropriate for FEM-simulations when several variables are studied, since these simulations can be very time-consuming.

The temperature control in the simulation models makes the size of the lesion relatively independent of the actual electric conductivity of the tissue. This would not be true if a constant effective voltage is applied to the electrode tip, in which case heating would increase with increasing electric conductivity. Nor would it be true if there were a large variation of the conductivity in the surrounding tissue, since this would alter the current density around the tip. Nearby cerebrospinal fluid, which has a much higher electric conductivity than the brain tissue (Duck 1990), might for instance lead the current away from the surrounding tissue and thus influence the heat generation (Cosman 1996).

Increased thermal conductivity of the tissue dissipates heat faster into the surrounding tissue. This will result in a larger lesion if temperature control compensates for the conductive heat loss around the electrode. It is worth noting that applying the effective conductivity equation without coagulation dependence would increase the size of the simulated lesion when blood perfusion increases, since it models blood perfusion as an increased thermal conductivity (Wren et al. 2001a) and the quadratic regression model gives increased lesion size with increased  $k_{tiss}$  (Fig. 5). By reducing the thermal

conductivity in coagulated tissue, as in Equation (6), increased blood perfusion decreases the size of the simulated lesion instead. Less heat will be conducted from the closest vicinity of the tip compared to the amount of heat conducted from non-coagulated tissue and the coagulated tissue will thus act as thermal insulation (Fig 2a). The latter model is supported by experimental studies of lesions made in liver with a similar temperature control as in this study (Aschoff et al. 2001), or with internal cooling of the electrode (Goldberg et al. 1998). Increased blood perfusion decreased lesion size in both cases. Thus, unless the coagulation of blood vessels is taken into consideration, the effective conductivity equation might not be suitable when it is used to simulate the creation of a lesion. Similar modifications of the impact of blood perfusion have been used by others for Pennes' bio-heat equation (Chang and Nguyen 2004) and are probably necessary if some other heat conduction equation, e.g. the Hybrid equation described in (Wren et al. 2001b), is used.

The simulation results appear realistic compared to the lesion volumes and diameters extracted from our group's earlier *in vivo* study on porcine brain (Eriksson et al. 2002) although appropriate values for  $k_{perf}$  are not known in detail. In the present study additional analysis was performed where the volume of two lesions (70 and 80 °C) from the Eriksson 2002 material was calculated by summing the areas of 100- $\mu$ m cryosectioned and Nissl colour stained slices to a volume. The volume and diameter of the experimental 70 °C lesion was 15.0 mm<sup>3</sup> (17.8 mm<sup>3</sup> if the volume of the hole from the electrode is included) and 2.7 mm respectively. This is comparable with a low or mean level of  $k_{tiss}$  and a mean blood perfusion level ( $k_{perf}$ ), alternatively a mean or high level of  $k_{tiss}$  and a high level of  $k_{perf}$  (Table IV). The volume and diameter of the experimental 80 °C lesion was measured to 35.4 mm<sup>3</sup> (39.5 mm<sup>3</sup> if the volume of the hole from the electrode is included) and 3.8 mm respectively. Compared to the results in Table IV this would be comparable with a low level of  $k_{tiss}$  and a mean level of  $k_{perf}$  or a high level of  $k_{tiss}$  and a high level of  $k_{perf}$ .

An experimental comparison between lesion size and laser Doppler perfusion monitoring may elucidate the impact of blood perfusion even further. A system with an RF-electrode

using optical fibres for laser Doppler measurements of microvascular perfusion during lesioning has been developed and evaluated by us and co-workers (Antonsson et al. 2005), (Antonsson et al. 2006). It would also be of interest to investigate heterogeneous surrounding tissue, such as the presence of large blood vessels, bone or cerebrospinal fluid within a few mm of the electrode tip. In such studies the assumption of axial symmetry would generally be invalid, thereby requiring three-dimensional modelling adding numerical complexity and requiring considerably more computational power. The use of effective thermal conductivity through  $k_{perf}$  assumes that the direction of flow differs in individual adjacent vessels and that there is no large bulk directionality in the blood perfusion (Arkin et al. 1994). This is probably not entirely correct but should be the best approximation when bulk directionality is not known. Directionality of blood flow would be another interesting subject to study in the future.

In conclusion, the results from this study show that the coagulation dependence of the thermal conductivity greatly altered the impact of blood perfusion in the simulations. Increased thermal conductivity of the tissue increased lesion size while increased blood perfusion decreased the lesion size in the simulations. Due to interactions, which were found when using the factorial design, these effects were strengthened with an increasing preset temperature. The ultimate goal of using simulations is design of a patient specific pre-planning neurosurgical tool, and thus even further studies are necessary.

### **Acknowledgment**

The authors would like to thank Prof. Eva Enqvist, Department of Mathematics, Linköping University, for her interest and valuable aid with the statistical design and analysis.

## Tables

*Table I. Physical properties of the different materials. a: Source: (Foster and Schwan 1989) (0.17-0.21 S/m, 37 °C in vitro) and (Latikka et al. 2001) (0.28 S/m, in vivo), b: Source: (Duck 1990). The value of  $3.6 \cdot 10^3$  J/(kg·K) was used for the specific heat of the grey matter. c: Source: (Chato 1985), d: Source: (Holman 2001), e: Source: (Nordling and Österman 1996)*

	electric conductivity, $\sigma$ (S/m)	mass density, $\rho$ (kg/m <sup>3</sup> )	specific heat capacity, $c$ (J/(kg·K))	thermal conductivity, $k$ (W/(m·K))
grey matter	0.17-0.28 <sup>a</sup>	$1.04 \cdot 10^3$ <sup>b</sup>	$3.6-3.7 \cdot 10^3$ <sup>b</sup>	0.16-0.57 <sup>c</sup>
stainless steel	- (Not used)	$7.9 \cdot 10^3$ <sup>d</sup>	$0.5 \cdot 10^3$ <sup>d</sup>	15 <sup>d</sup>
air	- (Not used)	1.3 <sup>e</sup>	$1.0 \cdot 10^3$ <sup>e</sup>	0.026 <sup>e</sup>
plastic layer	- (Not used)	$1.3 \cdot 10^3$ <sup>d</sup>	$2.16 \cdot 10^3$ <sup>d</sup>	0.25 <sup>d</sup>

*Table II. Levels used in the simulations. Only high and low levels were used for the 2<sup>4</sup>-factorial design. <sup>a</sup>The electric conductivity is given at 20 °C and is thus lower than in Table I.*

	$\sigma$ (S/m) <sup>a</sup>	$k_{tiss}$ (W/(m·K))	$k_{perf}$ (W/(m·K))	$T_{set}$ (°C)
low level (-1)	0.130	0.200	0	70
semi-low level (-0.5)	not used	0.275	0.125	75
mean level (0)	0.175	0.350	0.250	80
semi-high level (+0.5)	not used	0.425	0.375	85
high level (+1)	0.220	0.500	0.500	90

Table III.  $2^4$ -factorial design and resulting volumes and diameters with the contrast coefficients for low level (-1) and high level (+1). The mean level (0) was used to verify the linear model obtained by the rest of the simulations.

$c_\sigma$	$c_{ktiss}$	$c_{kperf}$	$c_{Tset}$	Volume (mm <sup>3</sup> )	Diameter (mm)
-1	-1	-1	-1	25.1	3.2
+1	-1	-1	-1	25.1	3.2
-1	+1	-1	-1	32.0	3.3
+1	+1	-1	-1	32.0	3.4
-1	-1	+1	-1	10.8	2.3
+1	-1	+1	-1	12.1	2.3
-1	+1	+1	-1	16.1	2.7
+1	+1	+1	-1	15.2	2.6
-1	-1	-1	+1	90.0	5.1
+1	-1	-1	+1	92.6	5.1
-1	+1	-1	+1	116.7	5.6
+1	+1	-1	+1	123.7	5.8
-1	-1	+1	+1	35.2	3.6
+1	-1	+1	+1	36.6	3.7
-1	+1	+1	+1	61.2	4.4
+1	+1	+1	+1	63.6	4.5
0	0	0	0	40.2	3.8

Table IV. Design matrix used in the quadratic regression analysis, Eq. (8), and resulting volumes and diameters. Results best agreeing with the experiments are marked with \* for  $T_{set} = 70\text{ }^{\circ}\text{C}$  and \*\* for  $T_{set} = 80\text{ }^{\circ}\text{C}$ . ( $c_0$  is a column of ones needed to calculate the regression coefficients.)

$c_0$	$c_{Tset}$	$c_{ktiss}$	$c_{kperf}$	Combinations of $c_{Tset}$ , $c_{ktiss}$ and $c_{kperf}$	$c_{ktiss}^2 \cdot c_{kperf}^2$	Volume ( $\text{mm}^3$ )	Diameter (mm)
+1	-1	-1	-1	.....	+1	25.1	3.2
+1	-1	-1	-1	.....	+1	25.1	3.2
+1	0	-1	-1	.....	+1	58.5	4.2
+1	0	-1	-1	.....	+1	60.6	4.3
+1	+1	-1	-1	.....	+1	90.0	5.1
+1	+1	-1	-1	.....	+1	92.6	5.1
+1	-1	0	-1	.....	0	26.1	3.3
+1	0	0	-1	.....	0	65.7	4.6
+1	+1	0	-1	.....	0	108.9	5.5
+1	-1	+1	-1	.....	+1	32.0	3.3
+1	-1	+1	-1	.....	+1	32.0	3.4
+1	0	+1	-1	.....	+1	70.9	4.7
+1	0	+1	-1	.....	+1	72.9	4.7
+1	+1	+1	-1	.....	+1	116.7	5.6
+1	+1	+1	-1	.....	+1	123.7	5.8
+1	-1	-1	0	.....	0	14.2*	2.6
+1	0	-1	0	.....	0	33.1**	3.5
+1	+1	-1	0	.....	0	50.5	4.2
+1	-1	0	0	.....	0	18.4	2.8
+1	0	0	0	.....	0	40.2	3.8
+1	+1	0	0	.....	0	69.8	4.7
+1	-1	+1	0	.....	0	22.8	3.0
+1	0	+1	0	.....	0	50.0	4.1
+1	+1	+1	0	.....	0	83.1	5.0
+1	-1	-1	+1	.....	+1	10.8	2.3
+1	-1	-1	+1	.....	+1	12.1	2.3
+1	0	-1	+1	.....	+1	22.2	3.0
+1	0	-1	+1	.....	+1	23.0	3.0
+1	+1	-1	+1	.....	+1	35.2	3.6
+1	+1	-1	+1	.....	+1	36.6	3.7
+1	-1	0	+1	.....	0	13.9*	2.3
+1	0	0	+1	.....	0	28.6	3.4
+1	+1	0	+1	.....	0	50.2	4.2
+1	-1	+1	+1	.....	+1	16.1*	2.7
+1	-1	+1	+1	.....	+1	15.2*	2.6

+1	0	+1	+1	.....	+1	37.2**	3.7
+1	0	+1	+1	.....	+1	38.0**	3.7
+1	+1	+1	+1	.....	+1	61.2	4.4
+1	+1	+1	+1	.....	+1	63.6	4.5
+1	-0.5	-0.5	-0.5	.....	+0.0625	33.1	3.5
+1	+0.5	-0.5	-0.5	.....	+0.0625	61.8	4.4
+1	-0.5	+0.5	-0.5	.....	+0.0625	38.6	3.7
+1	+0.5	+0.5	-0.5	.....	+0.0625	73.3	4.8
+1	-0.5	-0.5	+0.5	.....	+0.0625	23.0	3.0
+1	+0.5	-0.5	+0.5	.....	+0.0625	39.5	3.8
+1	-0.5	+0.5	+0.5	.....	+0.0625	24.9	3.2
+1	+0.5	+0.5	+0.5	.....	+0.0625	52.5	4.2

### Legends to figures

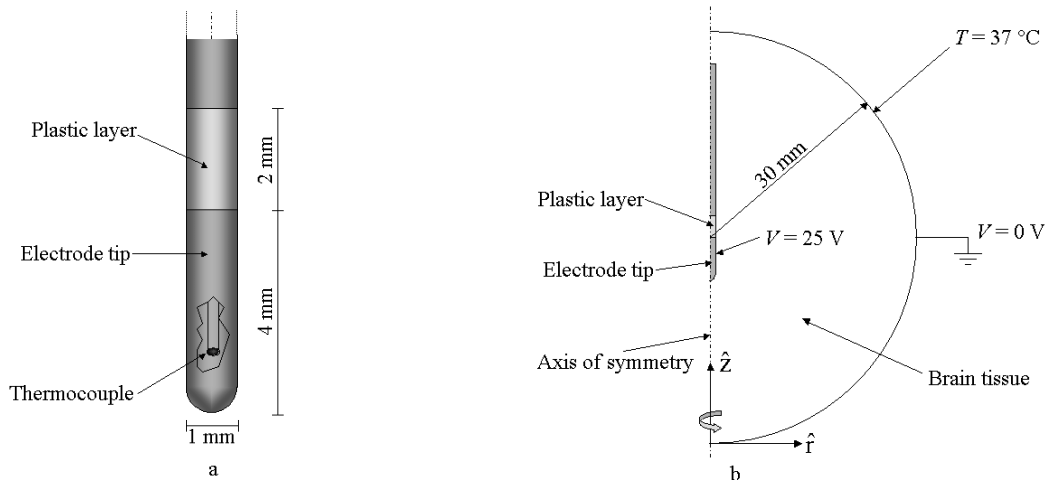


Fig. 1: (a) The active part of the brain electrode. The current goes from the tip to a much larger neutral plate, causing resistive heating of the tissue around the tip. The tissue then heats the tip whose temperature is measured by an embedded thermocouple. The measured temperature,  $T_{tip}$ , is then used to control the current. (b) Computer model; geometry and boundary conditions. Axial symmetry of the electrode and the surrounding tissue reduces the problem to two dimensions.

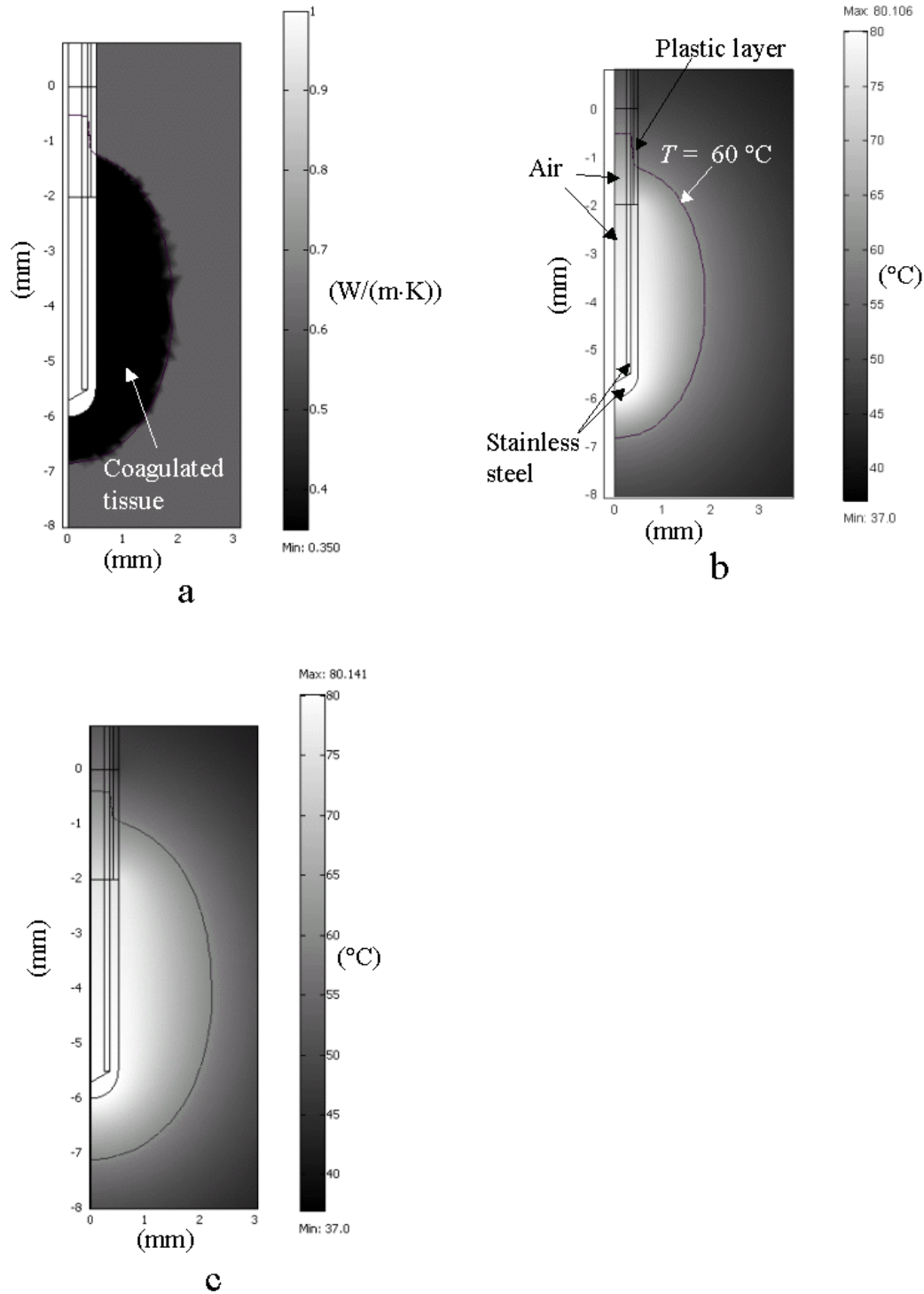


Fig. 2: (a) The effective thermal conductivity of the tissue. As the tissue coagulates the blood perfusion ceases and the coagulum becomes thermally insulating compared to the surrounding tissue thus focussing the heat to the already coagulated tissue. (b) Example of the temperature field after 60 s zoomed around the tip. The lesion is assumed to consist

of all tissue reaching a temperature of 60 °C or more. The 60 °C isotherm is marked with a black line. All variables in this simulation were set to the middle level:  $T_{set} = 80$  °C,  $\sigma = 0.175$  S/m,  $k_{tiss} = 0.35$  W/(m·K) and  $k_{perf} = 0.25$  W/(m·K). (c) Temperature field for a simulation with all variables set to middle level except for  $k_{perf} = 0$  W/(m·K). With no blood perfusion cooling the lesion becomes larger and here gets a volume of 65.7 mm<sup>3</sup> compared to 40.2 mm<sup>3</sup> in (b).

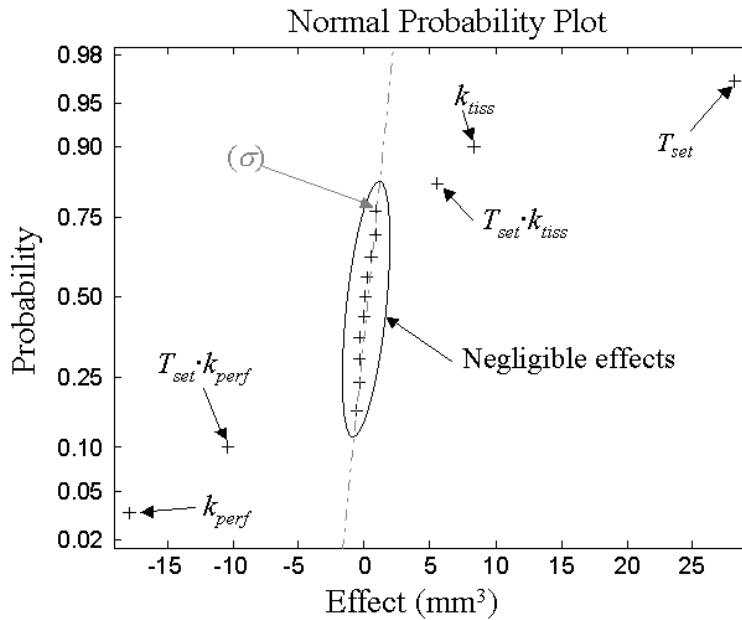


Fig. 3: Normal probability plot for effects from the 2<sup>4</sup>-factorial design with effects sorted from largest negative to largest positive. The plot is scaled in such a way that unimportant effects, here  $\sigma$  and most parameter interactions as indicated by the encircled area, will align themselves in a line. Important effects such as  $T_{set}$ ,  $k_{perf}$  and their interaction will however stand out from this line.

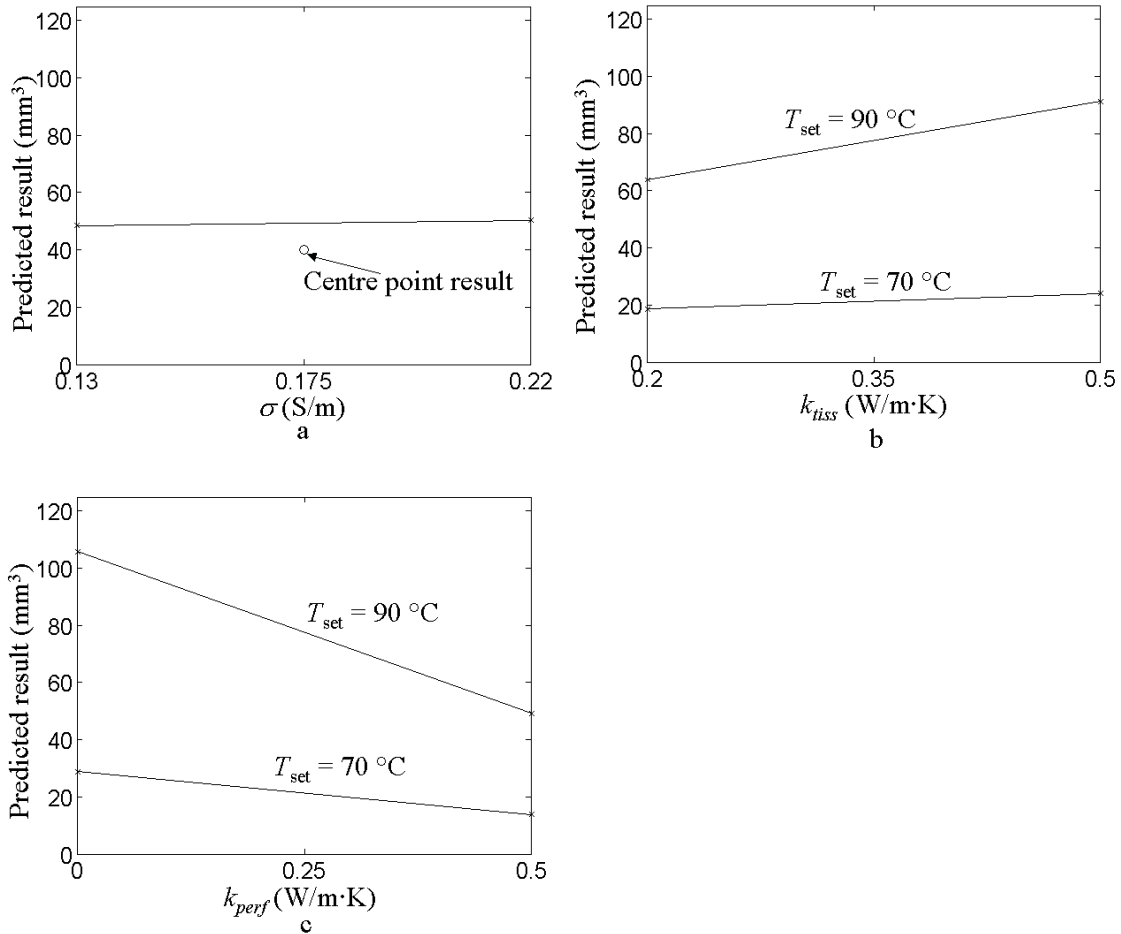


Fig. 4: Effect plots for the  $2^4$ -factorial design. (a)  $\sigma$  has little effect and is thus neglected in the linear regression model. The result for the centre point simulation should be close to the line if the linear regression model is sufficient. The result deviates noticeably however (about 9 mm<sup>3</sup>) which indicates that higher order terms may improve it. (b) Influence and interaction of  $k_{tiss}$  and  $T_{set}$ . The predicted lesion volume increases with  $k_{tiss}$ , especially for high  $T_{set}$ . (c) Influence and interaction of  $k_{perf}$  and  $T_{set}$ . The impact is larger with high  $T_{set}$  also for  $k_{perf}$ .

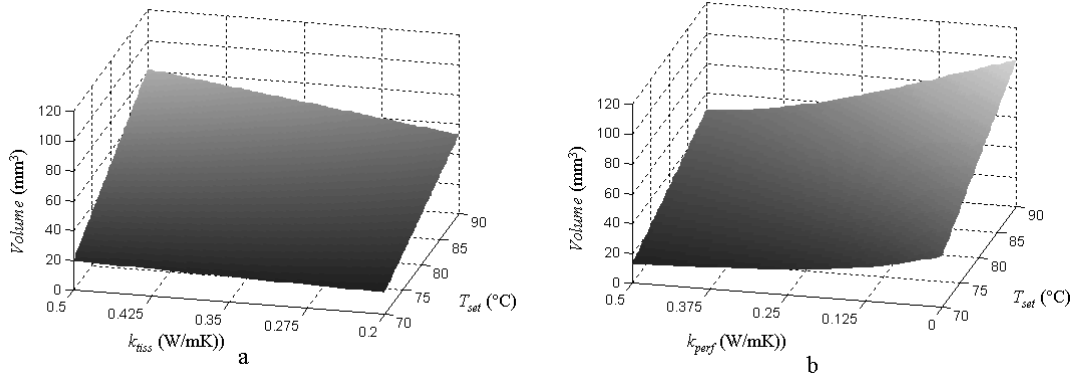


Fig. 5: Response surfaces of the lesion volume based on the quadratic regression model (8). Interaction between  $T_{set}$  and  $k_{tiss}$  is seen in (a) and interaction between  $T_{set}$  and  $k_{perf}$  is seen in (b). The main difference compared to the model based on the  $2^4$ -factorial design is the curvature that can be seen in (b)

## References

- Antonsson J, Eriksson O and Wårdell K (2005) Radio frequency electrode system for optical lesion size estimation in functional neurosurgery, *Journal of Biomedical Optics*, 10:3, pp 1-6
- Antonsson J, Eriksson O, Lundberg P and Wårdell K (2006) Optical measurements during experimental stereotactic radiofrequency-lesioning, *Stereotact Funct Neurosurg*, *In press*
- Arkin H, Xu LX and Holmes KR (1994) Recent developments in modeling heat transfer in blood perfused tissues, *IEEE Transactions on Biomedical Engineering*, 41:2, pp 97-107
- Aschoff AJ, Merkle EM, Wong V, Zhang Q, Mendez MM, Duerk JL and Lewin JS (2001) How does alteration of hepatic blood flow affect liver perfusion and radiofrequency-induced thermal lesion size in rabbit liver?, *J Magn Reson Imaging*, 13:1, pp 57-63
- Carslaw HS and Jaeger JC (1959) *Conduction of heat in solids*, 2nd ed. Oxford University Press, Oxford
- Chang IA and Nguyen UD (2004) Thermal modeling of lesion growth with radiofrequency ablation devices, *BioMedical Engineering OnLine*, 3:27,
- Chato JC (1980) Heat transfer to blood vessels, *J Biomech Eng*, 102:2, pp 110-118
- Chato JC (1985) Selected thermophysical properties of biological materials In: Shitzer A and Eberhart R (eds) *Heat Transfer in Medicine and Biology, Analysis and Applications*, Vol. 2 Plenum Press, New York and London, pp 413-418
- Cheng DK (1989) *Field and wave electromagnetics*, Addison-Wesley Publishing Company, Inc., USA
- Cosman E (1996) Radiofrequency lesions In: Gildenberg PL and Tasker R (eds) *Textbook of Stereotactic and Functional Neurosurgery*, Quebecor Printing, Kingsport, pp 973-985
- De Salles AA, Brekhus SD, De Souza EC, Behnke EJ, Farahani K, Anzai Y and Lufkin R (1995) Early postoperative appearance of radiofrequency lesions on magnetic resonance imaging, *Neurosurgery*, 36:5, pp 932-937
- Duck AF (1990) *Physical properties of tissue*, The University Press, Cambridge
- Eriksson O, Wren J, Loyd D and Wårdell K (1999) A comparison between in vitro studies of protein lesions generated by brain electrodes and finite element model simulations, *Med Biol Eng Comput*, 37:6, pp 737-741
- Eriksson O, Backlund E-O, Lundberg P, Lindstam H, Lindström S and Wårdell K (2002) Experimental radiofrequency brain lesions: a volumetric study, *Neurosurgery*, 51:3, pp 781-788
- Foster KR and Schwan HP (1989) Dielectric properties of tissues and biological materials: a critical review, *Critical Reviews in Biomedical Engineering*, 17:1, pp 25-103
- Goldberg SN, Hahn PF, Halpern EF, Fogle RM and Gazelle GS (1998) Radio-frequency tissue ablation: effect of pharmacologic modulation of blood flow on coagulation diameter, *Radiology*, 209:3, pp 761-767
- Goldberg SN (2001) Radiofrequency tumor ablation: principles and techniques, *Eur J Ultrasound*, 13:2, pp 129-147

- Hariz MI and Hirabayashi H (1997) Is there a relationship between size and site of the stereotactic lesion and symptomatic results of pallidotomy and thalamotomy?, *Stereotact Funct Neurosurg*, 69:1-4, pp 28-45
- Holman JP (2001) *Heat transfer*, 9th ed. McGraw-Hill Book company
- Labonté S (1992) A theoretical study of radio-frequency catheter ablation, Ph.D., Carlton Institute for Electrical Engineering, University of Ottawa, Ottawa
- Latikka J, Kuurne T and Eskola H (2001) Conductivity of living intracranial tissues, *Physics in Medicine and Biology*, 46:6, pp 1611-1616
- Montgomery DC and Runger GC (1994) *Applied statistics and probability for engineers*, John Wiley & Sons, Inc., New York
- Montgomery DC (1996) *Design and analysis of experiments*, John Wiley & Sons, Inc., USA
- Nordling C and Österman J (1996) *Physics handbook for science and engineering*, 5th ed. Studentlitteratur
- Raaymakers BW, Kotte ANTJ and Lagendijk JJW (2000) How to apply a discrete vessel model in thermal simulations when only incomplete vessel data are available, *Phys Med Biol*, 45: pp 3385-3401
- Tungjitsukulmun S, Woo EJ, Cao H, Tsai JZ, Vorperian VR and Webster JG (2000) Finite element analyses of uniform current density electrodes for radio-frequency cardiac ablation, *IEEE Trans Biomed Eng*, 47:1, pp 32-40
- van den Berg J and van Manen J (1962) Graded coagulation of brain tissue, *Acta Physiol Pharmacol Neerlandica*, 10: pp 353-377
- Weinbaum S and Jiji L (1989) The matching of thermal fields surrounding counter-current microvessels and the closure approximation in the Weinbaum-Jiji equation, *Journal of Biomechanical Engineering*, 111, pp 271-275
- Wren J, Eriksson O, Wårdell K and Loyd D (2001a) Analysis of temperature measurement for monitoring radio-frequency brain lesioning, *Med Biol Eng Comput*, 39:2, pp 255-262
- Wren J, Karlsson M and Loyd D (2001b) A hybrid equation for simulation of perfused tissue during thermal treatment, *International Journal of Hyperthermia*, 17:6, pp 483-498